Simple ZnO Nanowires Patterned Growth by Microcontact Printing for High Performance Field Emission Device

ARTICLE *in* THE JOURNAL OF PHYSICAL CHEMISTRY C · APRIL 2011

Impact Factor: 4.77 · DOI: 10.1021/jp2019044

THE JOURNAL OF PHYSICAL CHEMISTRY C

ARTICLE

pubs.acs.org/JPCC

Simple ZnO Nanowires Patterned Growth by Microcontact Printing for High Performance Field Emission Device

Hyun Wook Kang,[†,‡] Junyeob Yeo,[‡] Jin Ok Hwang,[§] Sukjoon Hong,[‡] Phillip Lee,[‡] Seung Yong Han,[‡] Jin Hwan Lee,[‡] Yoon Soo Rho,[‡] Sang Ouk Kim,[§] Seung Hwan Ko,[*,‡] and Hyung Jin Sung[*,†]

[†]Center for Opto-Fluid-Flexible Body Interaction, Department of Mechanical Engineering, [‡]Applied Nano Technology and Science Lab, Department of Mechanical Engineering, and [§]Soft Nanomaterials Lab, Department of Material Science and Engineering, KAIST, 291 Daehak-ro, Yuseong-gu, Daejeon, Korea

Supporting Information

ABSTRACT: We present a novel and simple method for the patterned growth of ZnO nanowires (NWs) that combines (1) the direct patterning of ZnO nanoparticle (NP) seeds via microcontact printing and (2) subsequent low-temperature hydrothermal growth. The ZnO NPs can be patterned as seed layers for ZnO NW growth on various substrates including flexible polymer films. The NW geometry and configuration can be controlled by varying the printing conditions (time and pressure) and the hydrothermal reaction time. The "needleleaf-like" sharp-tipped ZnO NWs with a radially grown structure were examined at the pattern edges. To assess the possibility of high-performance electronic applications of the patterned ZnO NWs, their field emission characteristics were examined by fabricating a high-performance field emission device with a patterned ZnO NW array. The remarkable enhancement of the field emission properties is attributed to the minimized field emission screening that results from the radial ZnO NW structures and micropatterning. This versatile ZnO NW patterning process is a powerful means for the large-scale and continuous production of functional ZnO NW devices.

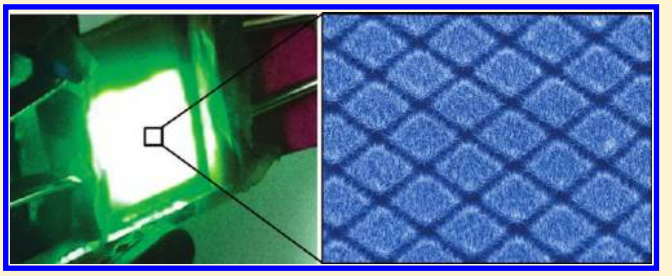

1. INTRODUCTION

The range of applications of nanomaterials is expanding into many fields such as electronics, biology, nanomachinery, and chemistry. One-dimensional (1D) nanostructures (nanowires, nanorods) with large surface−volume ratios and high sensitivity due to their highly anisotropic configurations are a particular area of intense research.[1] Zinc oxide nanowires (ZnO NWs) are among the most promising materials for the realization of useful nanoscale devices because of their ease of synthesis in the form of 1D nanostructures,[2] their unique properties such as a direct wide band gap (3.37 eV), piezoelectric characteristics, high sensitivity and selectivity for chemical and optical species, and the specific electrical and optical properties of a semiconductor with a large excitation binding energy (60 meV).[3,4] These unique properties of ZnO NWs mean that they have proven useful in photonic devices,[5] light-emitting diodes,[6] field-emission devices,[7−12] nanogenerators,[3] field-effect transistors,[13] UV lasers,[14] photovoltaic devices,[2,15,16] and chemical sensors.[17,18] However, in order to obtain more practical ZnO NW based devices, simple and economical techniques that enable periodic or arbitrary position control through localized pattern growth, large-scale fabrication, diverse substrate selectivity, and mass production are essential.

Various synthetic methods have been developed for the growth and fabrication of ZnO NWs; these methods can be classified into two categories: vapor-phase and hydrothermal syntheses. Vapor-phase synthetic methods include vapor−solid growth (VS),[4,10] vapor−liquid−solid growth (VLS),[19,20] chemical vapor deposition (CVD),[21] thermal evaporation,[22] and thermal decomposition and are generally used because of their expediency and the high quality of the resulting NWs. However, the vapor-phase synthetic method has some drawbacks such as high-process temperatures (700−900 °C), expensive equipment setup, and the difficulties of process control, which limit the large-scale fabrication, substrate selectivity, and mass production of these methods and are obstacles to the development of potential applications. In contrast, the development of hydrothermal synthetic methods widens the range of ZnO NW applications because of their low-process temperatures (below 100 °C), low cost, the possibility of scale-up, and simple process setup.[15,16] Various technologies for the localized pattern growth of ZnO NWs have been developed. In most vapor-phase syntheses of ZnO NWs, Au catalysts are used. Thus when patterned ZnO NW growth is desired, Au catalyst patterning techniques such as nanosphere lithography,[5] template methods,[23] laser interference lithography,[24] and atomic force

Received: February 27, 2011
Revised: May 11, 2011
Published: May 23, 2011

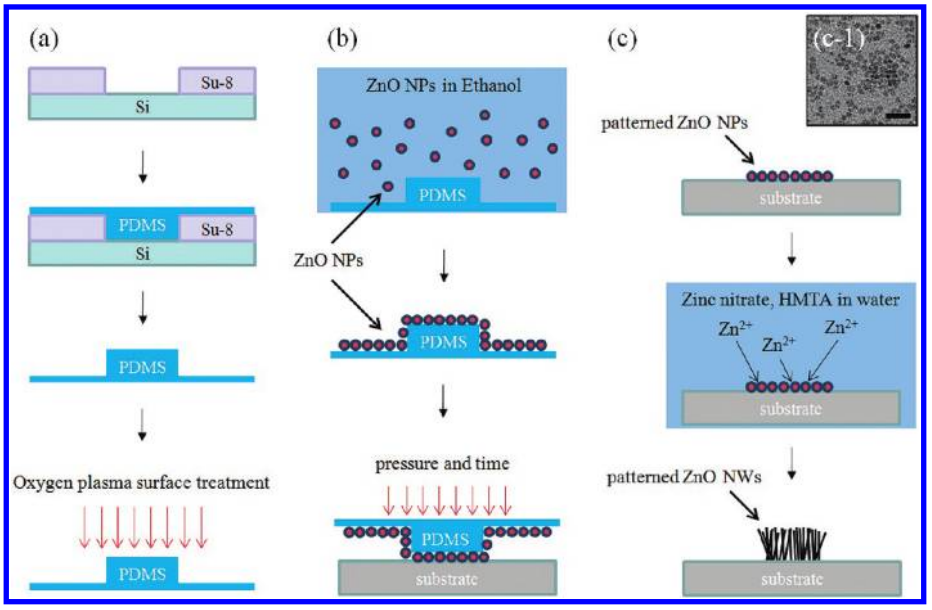

Figure 1. Schematic diagrams of the ZnO NW patterned growth process: the direct printing of the ZnO NP seed layer and subsequent low-temperature ZnO NW hydrothermal local growth on the printed ZnO NP seeds. (a) μCP stamp preparation: elastomeric polymer (PDMS) stamp replication from a SU-8 pattern prepared with conventional photolithography and oxygen plasma surface treatment. (b) ZnO NP seed layer patterning: the adhesion of ZnO NPs to the PDMS stamp surface and subsequent transfer (printing) to the target substrate. (c) ZnO NW local growth: the hydrothermal growth of patterned ZnO NWs on the previously printed ZnO NP seed pattern from an aqueous solution containing zinc nitrate hydrate, HMTA and PEI. (c-1) TEM image of ZnO NP seeds (scale bar = 15 nm).

microscopy (AFM) nanomachining[25] are required. However, vapor-phase synthesis methods need high-process temperatures that can damage substrates and connected metal electrodes. Furthermore, Au catalyst patterning is complicated, expensive, difficult to apply to large-scale and arbitrary shape fabrication, and the catalyst particle remains on the NW tip. ZnO nuclei synthesized via the thermal decomposition of zinc acetate ($Zn(OAc)_2$) have been employed instead of Au catalysts in hydrothermal and some vapor-phase ZnO NW syntheses. To pattern the ZnO seed layer, conventional photolithography,[26,27] e-beam lithography,[28] a microfluidic channel,[29] and inkjet printing[30] have been used. However, the thermal decomposition process for ZnO seed generation requires high-process temperatures (>300 °C) that are not acceptable for plastic substrates and involves several steps including a photoresist removal process. In addition, the control required to fabricate a uniformly distributed ZnO seed layer and a sharp pattern edge is difficult to achieve. Self-assembled monolayers (SAMs) have also been employed in ZnO NW patterning processes with chemically modified surfaces.[6,31,32] The functional end groups (carboxylic acid) of thiol species interact with the cationic zinc ions in the zinc acetate solution and act as a seed layer for ZnO NW growth. The SAM patterning process has some disadvantages, because it can only be applied to a limited range of substrate materials (Au, Ag), and the unpatterned surface must be chemically modified. Despite various attempts to extend their range, most ZnO NW patterning approaches have limited applications due to their requirements of additional chemical processing and particular materials.

In this study, we developed a simple and novel ZnO NW patterning technique that uses direct seed material pattern printing and low-temperature hydrothermal synthesis. In this ZnO NW synthesis method, ZnO quantum dots are employed as the seed material and are patterned with a microcontact printing method. Our method is a low-temperature process that does not require vacuum deposition and is a dramatic simplification of existing patterned ZnO NW array preparation processes. By varying the printing conditions (time and pressure) and the hydrothermal reaction time, the ZnO NW geometries can be controlled. The resulting optimized ZnO NW patterns exhibit considerably improved field emission performance due to the screening effect reduction by radially grown ZnO NWs and micropatterning.

2. EXPERIMENTAL METHODS

Elastomeric Polymer Stamp Preparation. A silicon (Si) wafer (Siltron, Inc.) was preheated at 100 °C for 20 min then cleaned with oxygen plasma surface treatment at 200 mTorr and 100 W for 60 s. A 10 μm thick film of SU-8 (Micro Chem) negative photoresist (PR) was spin-coated onto the Si wafer, and UV exposed through a photomask at 100 mJ. The SU-8 thin film was developed to yield the pattern and then cleaned with isopropyl alcohol and deionized (DI) water. An elastomeric polymer, polydimethylsiloxane (PDMS) (SYLGARD 184 Silicone Elastomer KIT, Dow Corning), was poured onto the SU-8 mold and cured at 60 °C for 1 h. After the curing process, the PDMS was detached from the SU-8 mold and prepared as an elastomeric polymer stamp for the μCP process.

Substrate Preparation. A Si wafer with a 300 nm thick SiO_2 layer was prepared by using wet oxidation. A 5 μm thick titanium film adhesion promotion layer and a 30 μm thick gold film were deposited on the SiO_2/Si wafer as a metal electrode via e-beam evaporation. Glass substrates (Fisher Scientific) were cleaned with the following procedure: sonication in a 1:1 solution of ethanol and DI water, rinsing in acetone, rinsing in DI water, and drying with nitrogen gas. Polyethylene terephthalate (PET) and polyimide (PI) were used as flexible substrates.

ZnO Seed NP Synthesis. Thirty millimolar sodium hydroxide (NaOH, Sigma Aldrich) and 10 mM zinc acetate ($Zn(OAc)_2$, Sigma Aldrich) in ethanol were reacted at 60 °C for 2 h and cooled at room temperature.

Precursor Preparation for ZnO NW Hydrothermal Synthesis. An aqueous solution of 25 mM zinc nitrate hexahydrate ($Zn(NO_3)_2 \cdot 6H_2O$, Sigma Aldrich), 25 mM hexamethylenetetramine (HMTA, $C_6H_{12}N_4$, Sigma Aldrich), and 5−7 mM polyethylenimine (PEI, C_2H_5N, Sigma Aldrich) was heated at 95 °C for 1 h and cooled to room temperature.

Field Emission Measurements. A gold-coated highly doped n-type Si wafer with patterned ZnO NW arrays was utilized as the cathode electrode. The anode electrode was prepared by screen printing a phosphor (ZnS/Ag,Cl) onto a 100 nm thick ITO-coated glass substrate. The spacing between the anode and the cathode was maintained at 100 μm. The field emission characteristics were measured by applying a voltage of 0−5000 V between the two electrodes in a vacuum ($\sim 10^{-6}$ Torr) environment.

3. RESULTS AND DISCUSSION

Our method for simple ZnO NW patterned growth consists of the three stages shown in Figure 1: (1) elastomeric mold fabrication for microcontact printing (μCP), (2) ZnO seed nanoparticle direct patterning by using μCP, and (3) subsequent selective hydrothermal ZnO NW growth on the microcontact printed ZnO NP seeds. The μCP technique is based on molding and embossing with an elastomeric stamp and has been successfully applied to the modification of surfaces with various textures.[33,34] μCP can easily be applied to curved or arbitrary configurations, as well as to microelectromechanical system devices, cell biology, microfluidics, flexible electronics, and photonics.

An elastomeric stamp obtained with the soft lithography technique was applied to fabricate patterned ZnO NP seed layers. As shown in Figure 1a, a SU-8 PR was spin-coated, then exposed and developed on a Si wafer to fabricate a rigid master mold. A PDMS stamp was used as the elastomeric stamp; it was cast from an SU-8 mold then cleaned with oxygen plasma surface treatment. The plasma-treated PDMS stamp was immersed in ZnO quantum dots (3−4 nm, a TEM image of the ZnO NPs is shown in Figure 1c-1) in ethanol solution for 1 min and dried with nitrogen gas at room temperature. The ZnO quantum dots adhere to the PDMS stamp surface and act as seed particles for ZnO NW growth. The substrates on which the ZnO NPs are patterned for ZnO NW growth were prepared with the appropriate cleaning process (see Section 2, Substrate Preparation). Si, SiO_2, glass, gold, PET, and PI were used as substrates without any additional surface treatments such as PR coating, SAM treatment, mask contact, or oxygen plasma surface treatment.

The ZnO NPs for use as seeds in ZnO NW local growth are printed from the PDMS stamp surface onto the substrate surface by the molecular diffusion induced by the direct contact of the surfaces. The most important parameters for the printing of uniform ZnO NP seed patterns and the avoidance of air bubble trapping by irregular contact were found to be printing pressure and printing time. As the printing time increases, the ZnO NP seeds diffuse further, which results in the growth of ZnO NWs over a larger area and with a larger number density (Supporting Information Figure S1). When the printing pressure is increased above a critical value, the effects of the sagging of the compliant PDMS mold under high pressure become dominant and unintentional ZnO NW growth is observed (Supporting Information Figure S2). The optimum printing pressure was found to be 0.03−0.2 psi and the printing time was controlled in the range 10−100 s to maximize the resolution and fidelity of the printed pattern and prevent unintentional growth (Figure 1b).

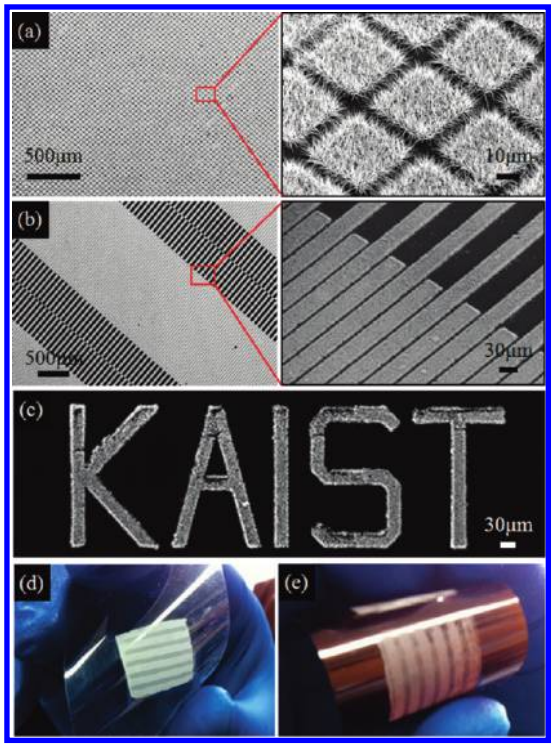

Figure 2. SEM images and photographs of ZnO NW patterned growth. Large-area ZnO NW local growth on (a) a square pattern array (area 30 × 30 μm^2 and pitch 5 μm), and (b) an interdigitated line pattern array (line width 30 μm with pitches 5 μm in the dense region and 40 μm in the coarse region). The images on the right show magnified views of the regions enclosed in red boxes (a,b). (c) SEM image of ZnO NW local growth on an arbitrary letter pattern, "KAIST". Digital photographs of ZnO NW patterned growth on plastic substrates ((d) PET film and (e) PI film). The stripes result from the difference in pattern density (d,e).

A substrate with patterned ZnO NP seeds was immersed in aqueous solutions containing 25 mM $Zn(NO_3)_2 \cdot 6H_2O$, 25 mM HMTA, and 5−7 mM PEI at 95 °C for 5−12 h. After the growth process was completed, ZnO NWs were found to have grown only on the printed ZnO NP seeds on the substrate; they were then rinsed with ethanol and dried in nitrogen gas (Figure 1c). The patterned ZnO NW growth arrays on the μCP ZnO NP seeds are shown in Figure 2. Fine ZnO NWs clearly patterned over a large area (up to $\sim$10 cm^2) were successfully demonstrated. Figure 2a,b shows scanning electron microscope (SEM) images of patterned ZnO NWs grown on a square array (area, 30 × 30 μm^2; pitch, 5 μm) and on an interdigitated line pattern array (width, 30 μm; pitches, 5 and 40 μm), respectively. As shown in Figure 2, the fidelity of the local ZnO NW patterned growth is very high without any residuals or unselectively grown ZnO NWs over a large area. This process provides high flexibility in design and substrate selection. Arbitrary patterns can easily be achieved through PDMS stamp design modification, as shown in Figure 2c. The low temperatures used in our proposed process enable the use of temperature-sensitive substrates and materials.

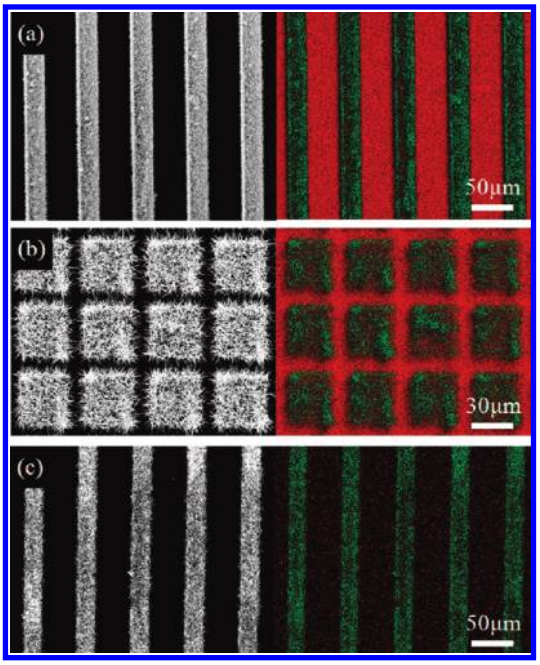

Figure 3. SEM-EDX analysis of ZnO NW patterned growth. (a) Array of microlines (width, 40 μm; pitch, 20 μm) on a Si wafer (520 μm thick), green dots, ZnK (elemental zinc); red dots, SiK (elemental silicon). (b) Array of microsquares (area, 30 × 30 μm^2, pitch, 5 μm) on a SiO_2 wafer (300 nm thick); green dots, ZnK (elemental zinc); red dots, SiK (elemental silicon). (c) Array of microlines (width, 40 μm; pitch, 20 μm) on a gold-coated surface (30 nm thick); green dots, ZnK (elemental zinc); red dots, AuM (elemental gold).

ZnO NW patterned growth was also demonstrated on flexible substrates, as shown in Figure 2d (PET film) and Figure 2e (PI film). The stripes in the grown ZnO NWs result from a difference in pattern density. The large degree of freedom of substrate selection and the versatility of ZnO NW pattern fabrication extend the range of ZnO NW applications, in particular to flexible electronics and photonics.

Local pattern fidelity without unintentional ZnO NW growth or a residual layer is very important for high-performance electronic applications. Figure 3 shows SEM and energy-dispersive X-ray spectroscop(SEM-EDX) images that demonstrate the high fidelity of the ZnO NP seed printing and the subsequent ZnO NW local growth: (a) a ZnO NW line pattern array (width, 20 μm; pitch, 40 μm) on a Si wafer (520 μm thick) and (b) a ZnO NW square pattern array (area, 30 × 30 μm^2; pitch, 5 μm) on a SiO_2 wafer (300 nm thick). The EDX mapping of elemental zinc shows that the ZnK signals in the EDX spectra are present only in the patterned region (green dots indicate ZnK (elemental zinc) and red dots indicate SiK (elemental silicon)). Similar results were achieved for a gold-coated (50 nm thick) SiO_2 wafer (300 nm thick) with line patterns (Figure 3c, width, 20 μm; pitch 40 μm/green dots, ZnK; red dots, AuM (elemental gold)). The ZnO NWs have grown along the *c*-axis of the wurtzite crystal and have a hexagonal cross-section.

The transmission electron microscopy (TEM) images of individual ZnO NWs removed from the arrays indicate that they have a high quality single-crystalline structure and grew in the [001] direction (Figure 4a,b, TEM images; Figure 4a-1, b-1, selected area electron diffraction (SAED) pattern; Figure 4c, high-resolution TEM image). The development of this novel

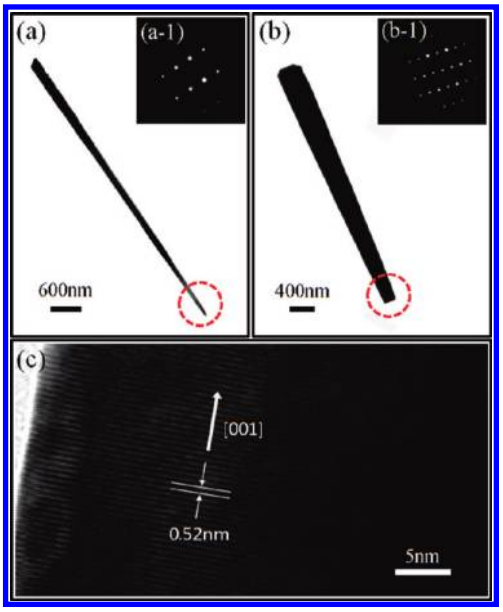

Figure 4. TEM images and SAED patterns of ZnO NWs. (a) TEM image of a ZnO NW grown for 12 h. (a-1) SAED pattern of 12 h grown ZnO NW. (b) TEM image of a ZnO NW grown for 5 h. (b-1) SAED pattern of 5 h grown ZnO NW. Note that longer reaction times produce longer ZnO NWs with sharper tips (the dotted circles indicate the tips of the NWs). (c) High-resolution TEM image.

NW direct local growth process enables the fabrication of various ZnO NW geometries. We now discuss several factors that can be controlled during the ZnO NW patterning and growth process. First, the length and tip shape of the ZnO NWs are governed by the reaction time. A single hydrothermal reaction process can produce 2−8 μm long ZnO NWs.[16] To grow ZnO NWs with lengths greater than 10 μm, multiple growth stages with fresh aqueous precursors are required. In addition, the shape of the ZnO NW tips can be controlled during the hydrothermal reaction. A truncated tip ZnO NW can be achieved when the reaction is stopped within 12 h. However, reaction times more than 12 h result in the formation of ZnO NWs with sharp tips due to the etching effect explained by the following reaction[12,35]

$$Zn^{2+} + NH_3 \cdot H_2O \rightarrow [Zn(NH_3)_4]^{2+} + OH^-$$

$$[Zn(NH_3)_4]^{2+} + 2OH^- \leftrightarrow ZnO + NH_3 + H_2O \quad (1)$$

An increase in the concentration of the intermediate compound $[Zn(NH_3)_4]^{2+}$ leads to ZnO formation following the thermal treatment of the precursor. In contrast, a decrease in the $[Zn(NH_3)_4]^{2+}$ concentration during the reaction induces ZnO dissolution. In this study, a growth time of 5 h was found to induce the formation of ZnO NWs approximately 2−5 μm in length with truncated tips (Figure 4b, Supporting Information Figure S4a), and a growth time of 12 h was found to induce the formation of ZnO NWs with lengths in the range 6−7 μm and sharp tips (Figure 4a, Supporting Information Figure S4b). Second, the diameters of the ZnO NWs can be controlled by capping polymer engineering. The addition of HMTA and PEI results in ZnO NWs with high-aspect ratios by allowing axial growth and preventing lateral growth. ZnO NWs grown from a precursor with 25 mM zinc nitrate hydrate, 25 mM HMTA, and

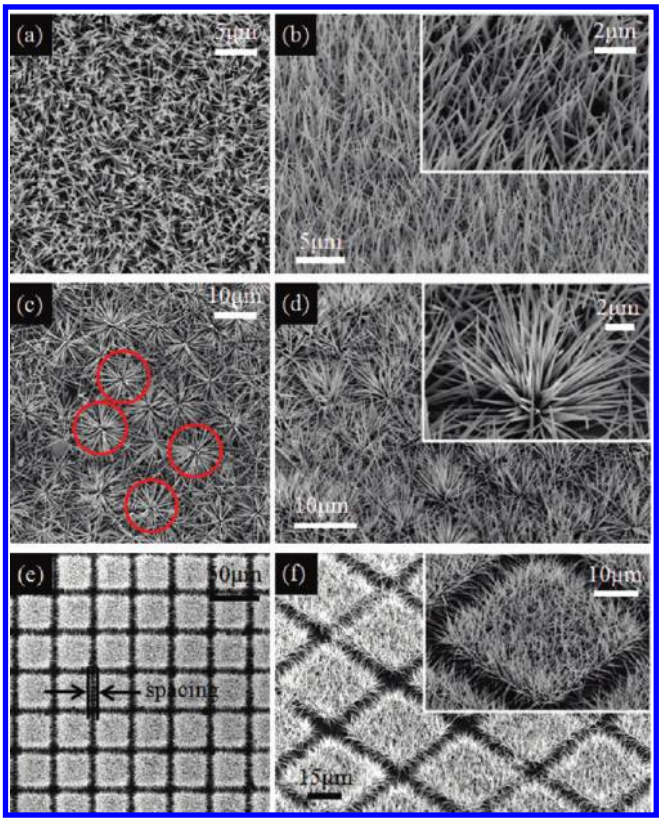

Figure 5. SEM images of ZnO NW arrays fabricated with two different printing times. A ZnO NW array with a printing time of 60 s: (a) top view and (b) 45° tilted view of the ZnO NW array grown vertically from ZnO seed NPs printed with a flat PDMS (no pattern) stamp. A ZnO NW array with a printing time of 30 s: (c) top view and (d) 45° tilted view of the ZnO NW array grown hemispherically from ZnO seed NPs printed with a flat PDMS stamp. The images in the insets show magnified views of the individual needleleaf-like ZnO NW arrays indicated by the red circles. (e) Top view and (f) 45° tilted view of a ZnO NW patterned growth array obtained from ZnO seed NPs printed on a PDMS square pattern with a printing time of 60 s. The spacing between the adjacent NW array elements is 5 μm. The printing pressure was maintained at 0.03 psi in all cases.

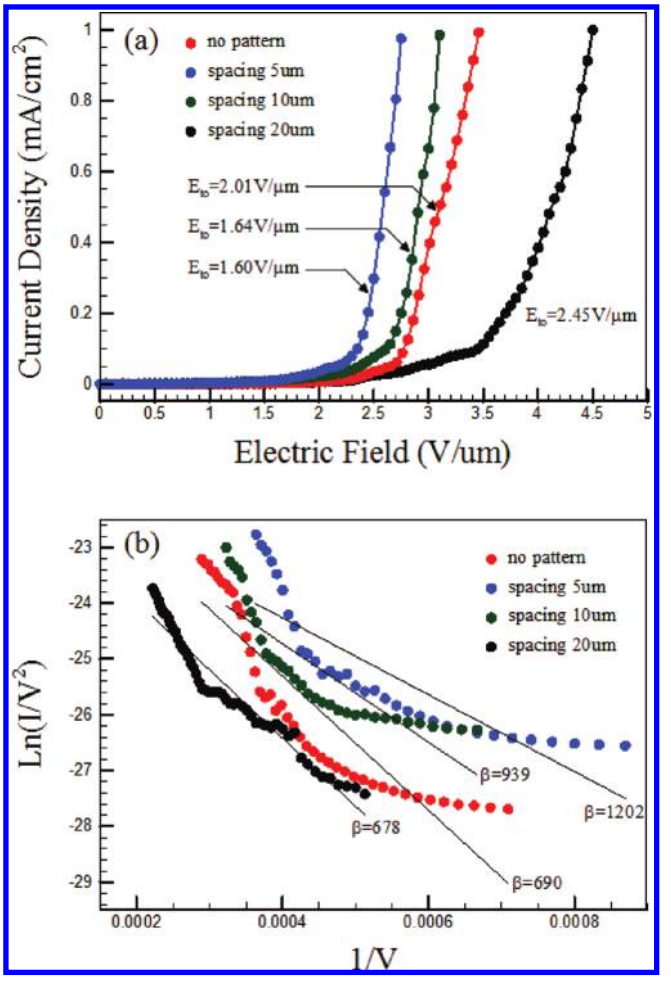

Figure 6. The field emission characteristics of ZnO NW square arrays with various configurations. (a) Current density versus applied electric field curves and (b) Fowler−Nordheim plots for a ZnO NW forest without pattern (using a flat PDMS stamp, red circles) and ZnO NW square patterns (30 × 30 μm^2) with various pattern spacings (5, 10, 20 μm).

5 mM PEI have diameters in the range 130−200 nm, whereas ZnO NWs grown from a precursor without PEI have much larger (0.8−2.5 μm) diameters (Supporting Information Figure S3). In addition, the location of the growth sites within the pattern and the growth time are other factors that can be used in the control of ZnO NW diameters. When the growth time is below 8−10 h, the diameters of the grown ZnO NWs are larger near the edge of the pattern (400−600 nm) than inside the pattern (100−200 nm). The dependence of the diameters of the NWs on location might be due to the effects of the density of neighboring NWs, which can hinder NW growth. The ZnO NWs grown at the edge might then have larger diameters because of a greater precursor chemical source supply than is present for the high density ZnO NWs in the central regions. However, this effect is eliminated when the growth time is longer than 12 h due to reaction termination and the initiation of etching (Supporting Information Figure S4). Third, the growth direction of the ZnO NWs can be controlled by varying the pattern geometry. The ZnO NWs grown at the edge of a pattern have a tendency to grow outward (in the low NW density direction), whereas the NWs at the central part of a pattern grow vertically. This effect becomes more serious when the pattern size is smaller than the lengths of the NWs, which results in the hemispherical growth of ZnO NWs from a point, as shown in Supporting Information Figure S1. Fourth, ZnO NW patterns with arbitrary shapes can be obtained by repeating the current printing process. The PDMS stamp can be used several times without requiring the additional treatment of seed material (Supporting Information Figure S5). With this approach, patterns with arbitrary shapes can be achieved by performing simple movements of a stage, and the continuous serial fabrication of ZnO NP seed patterned substrates can be used in mass production, such as in a roll-to-roll printing system.[36]

ZnO NW arrays with various geometries can be grown by combining the control of pattern shape and printing conditions. From a flat PDMS stamp without any pattern, two types of ZnO NW arrays can be fabricated. As shown in Figure 5a,b, vertically aligned ZnO NWs with a slight tilting angle were achieved with a printing (contact) time (pressure, 0.03 psi) longer than 60 s, which provides a uniform seed layer because it enables sufficient diffusion of the seed NPs. This result is very similar to those

described above. On the other hand, when the printing time is limited to 30 s, hemispherical growth "needleleaf-like" ZnO NW arrays with a diameter of ~10 μm were produced (Figure 5c,d). This growth mode could be due to a nonuniform seed layer, which will arise when the NP seed diffusion time is insufficient, and has a similar structure and origin to ZnO NWs grown at a pattern edge. The images in Figure 5e,f are of ZnO NW local growth on a square pattern array with a printing time of 60 s and show ZnO NWs produced by a combination of vertical and radial growth. In the image in the inset in Figure 5f, the ZnO NWs at the center of the square pattern have vertical growth structures and the ZnO NWs at the edge have radial growth structures.

The direct contact between the metal substrate and patterned ZnO NWs without chemical connection has advantages in various electronic applications. A field emission device is one application that can be realized with a metal electrode and ZnO NW array combination. Field emission screening effects need to be reduced to enhance field emission properties.[11,37] With this aim in mind, a needleleaf-like ZnO NW array without pattern (Figure 5b) and ZnO NW square patterned arrays with regular spacings (Figure 5c, pattern area, 30 × 30 μm^2; spacings, 5, 10, 20 μm) were prepared to study the effects of the ZnO NW patterning configuration on the field emission efficiency. The field emission performance was measured in a vacuum chamber with a pressure of 10^{-6} Torr at room temperature. The ZnO NW array cathode electrode for the field emission device (1 × 1 cm^2) was prepared on a gold-coated Si wafer (Au 30 nm, Ti 5 nm for the adhesion promotion layer), and phosphor (ZnS/Ag,Cl) was deposited on indium tin oxide (ITO) coated glass as an anode electrode (Figure 7a). Figure 7b shows a working field emission device fabricated with the current approach. In order to evaluate the field emission characteristics of the ZnO NW array configurations, a turn-on electric field (E_{to}) generating an emission current density of 10 μA cm^{-2} was applied and the electric field enhancement factors (β) calculated from Fowler–Nordheim (F-N) plots were measured and compared. Figure 6a presents the field emission current density versus applied field (J–E) curves. The E_{to} of the needleleaf-like ZnO NW array (no pattern) is 2.01 Vμm^{-1}, and the E_{to} of the ZnO NW square patterned array with a spacing of 5 μm is lower (1.60 V μm^{-1}). This E_{to} value is one of the best reported values for ZnO NW field emitters.[7−12] However, as the spacing within the ZnO NW square patterned arrays is increased, the E_{to} values increase (spacing 10 μm, 1.64 V μm^{-1}; spacing 20 μm, 2.45 V μm^{-1}) because the number of ZnO NW emitters decreases with the reduction in the ZnO NWs patterned area.

The electric field enhancement factors (β) were determined from the following equation and the slopes were obtained from the linear fitting of Figure 6b

$$\beta = \frac{B\Phi^{3/2}d}{\text{slope}}$$

(2)where B = 6.83 × 10^9 eV$^{-3/2}$ Vm^{-1}, Φ = 5.28 eV is the electron work function of ZnO, and d = 100 μm is the distance between the cathode and the anode. In general, β is related to the density, structure, and geometry of the emitters. The calculated β values of the ZnO NW square patterned arrays with spacings of 5, 10, and 20 μm are 1202, 939, and 678 respectively, whereas the calculated β value for the needleleaf-like ZnO NWs is 690. The higher β values of the ZnO NW square-patterned arrays might be due to the decreased field emission screening effects of the ZnO NW emitters. The microscale radial structure of ZnO NW arrays fabricated with micropatterning and printing time control might reduce the field emission screening effect because the tips of the ZnO NWs point in different radial directions and do not interfere with each other via screening. Even though the needleleaf-like ZnO NW array is an extreme case of a radial ZnO NW structure with zero spacing between the ZnO NW array domains, this array exhibits field emission characteristics that are inferior to those of the square patterned arrays. The ZnO NWs from two separate radial ZnO NW domains are sufficiently close that they screen the field emission characteristics, as shown in Figure 7c. On the other hand, when the space between the ZnO NWs from separate radial ZnO NW domains near the pattern edge is sufficiently large, the screening effect is minimized even as the advantages of radial ZnO NW arrays are retained (Figure 7d,e). This effect results in significant improvements in the field emission performance, even though the number of NW emitters decreases by the increased spacing between the patterns. However, further increase in the pattern spacing larger than 10 μm deteriorated the field emission performance drastically with increases in the pattern spacing by decreasing absolute number of ZnO NW emitters and pattern edge areas.

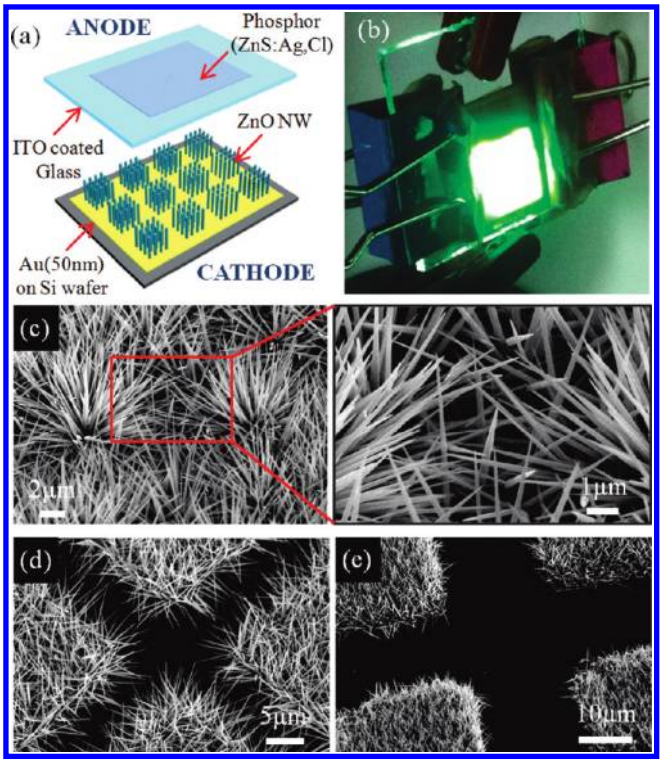

Figure 7. (a) A schematic illustration of a field emission device with a patterned ZnO NW array. (b) A luminous field emission device with a patterned ZnO NW array. (c) SEM images of two adjacent needleleaf-like ZnO NW arrays (the enlarged image shows the opposing ZnO NWs). SEM images of the edges of square ZnO NW patterned growth with (d) 5 μm spacing and (e) 20 μm spacing.

4. CONCLUSIONS

We have successfully demonstrated a novel and simple method for the patterned growth of ZnO NWs that combines (1) the direct patterning of ZnO NP seeds via microcontact printing and (2) subsequent low-temperature hydrothermal

ZnO NW selective growth on microcontact printed ZnO NP seeds. The growth of various ZnO NW patterns was successfully demonstrated on metal, inorganic, and plastic substrates without additional chemical treatment. This flexibility in substrate choice could enable the application of this approach to various fields such as flexible electronics and photonics that require ZnO NWs. The control of the ZnO NW geometries by varying the printing conditions (time and pressure) and the hydrothermal reaction time was successfully demonstrated. By using this control of pattern geometry and printing time, radially grown ZnO NW structures were created for use in the fabrication of an efficient field emission device. The optimum patterned ZnO NW field emission device fabricated with the current approach was found to exhibit a very low turn-on electric field value (1.60 μm V^{-1}), which is attributed to the decrease in the field emission screening effect that results from the radial structures of the micropatterned ZnO NW arrays. This versatile ZnO NW patterning process is expected to provide a powerful approach to the large-scale and mass production of functional ZnO NW application devices and could broaden the applications of ZnO NWs to biotechnology and energy related technologies.

■ ASSOCIATED CONTENT

Supporting Information. Detailed information on the ZnO NW growth on various printing conditions. This material is available free of charge via the Internet at http://pubs.acs.org.

■ AUTHOR INFORMATION

Corresponding Author
*E-mail: (S.H.K.) maxko@kaist.ac.kr; (H.J.S.) hjsung@kaist.ac.kr.

■ ACKNOWLEDGMENT

This work was supported by the Creative Research Initiatives (No. 2011-0000423)and Basic Science Research Program (2011-0005321) through the National Research Foundation (NRF) of Korea.

■ REFERENCES

(1) Gudiksen, M. S.; Lauhon, L. J.; Wang, J.; Smith, D. C.; Lieber, C. M. *Nature* **2002**, *415*, 617.
(2) Zhang, Q.; Dandeneau, C. S.; Zhou, X.; Cao, G. *Adv. Mater.* **2009**, *21*, 4087.
(3) Wang, Z. L.; Song, J. *Science* **2006**, *312*, 242.
(4) Wang, Z. L. *J. Phys.: Condens. Matter* **2004**, *16*, R829.
(5) Wang, X.; Summers, C. J.; Wang, Z. L. *Nano Lett.* **2004**, *4*, 423.
(6) Saito, N.; Haneda, H.; Sekiguchi, T.; Ohashi, N.; Sakaguchi, I.; Koumoto, K. *Adv. Mater.* **2002**, *14*, 418.
(7) Tseng, Y.-K.; Huang, C.-J.; Cheng, H.-M.; Lin, I.-N.; Liu, K.-S.; Chen, I.-C. *Adv. Funct. Mater.* **2003**, *13*, 811.
(8) Banerjee, D.; Jo, S. H.; Ren, Z. F. *Adv. Mater.* **2004**, *16*, 2028.
(9) Wang, W.; Zeng, B.; Yang, J.; Poudel, B.; Huang, J.; Naughton, M. J.; Ren, Z. *Adv. Mater.* **2006**, *18*, 3275.
(10) Yoon, H.; Seo, K.; Moon, H.; Varadwaj, K. S. K.; In, J.; Kim, B. *J. Phys. Chem. C* **2008**, *112*, 9181.
(11) Hwang, J. O.; Lee, D. H.; Kim, J. Y.; Han, T. H.; Kim, B. H.; Park, M.; No, K.; Kim, S. O. *J. Mater. Chem.* **2010**10.1039/C0JM01495H.
(12) Wang, C.; Yu, K.; Li, L.; Li, Q.; Zhu, Z. *Appl. Phys. A* **2008**, *90*, 739.
(13) Ko, S. H.; Park, I.; Pan, H.; Misra, N.; Rogers, M. S.; Grigoropoulos, C. P.; Pisano, A. P. *Appl. Phys. Lett.* **2008**, *92*, 154102.
(14) Huang, M. H.; Mao, S.; Feick, H.; Yan, H.; Wu, Y.; Kind, H.; Weber, E.; Russo, R.; Yang, P. *Science* **2001**, *292*, 1897.
(15) Law, M.; Greene, L. E.; Johnson, J. C.; Saykally, R.; Yang, P. *Nat. Mater.* **2005**, *4*, 455.
(16) Ko, S. H.; Lee, D.; Kang, H. W.; Nam, K. H.; Yeo, J.; Hong, S.; Grigoropoulos, C. P.; Sung, H. J. *Nano Lett.* **2011**, *11*, 666.
(17) Ramgir, N. S.; Yang, Y.; Zacharias, M. *Small* **2010**, *6*, 1705.
(18) Youn, S. K.; Ramgir, N.; Wang, C.; Subannajui, K.; Cimalla, V.; Zacharias, M. *J. Phys. Chem. C* **2010**, *114*, 10092.
(19) Zacharias, M.; Subannajui, K.; Menzel, A.; Yang, Y. *Phys. Status Solidi B* **2010**, *247*, 2305.
(20) Fan, H. J.; Werner, P.; Zacharias, M. *Small* **2006**, *6*, 700.
(21) Ok, J. G.; Tawfick, S. H.; Juggernauth, K. A.; Sun, K.; Zhang, Y.; Hart, A. J. *Adv. Funct. Mater.* **2010**, *20*, 2470.
(22) Kar, S.; Pal, B. N.; Chaudhuri, S.; Chakravorty, D. *J. Phys. Chem. B* **2006**, *110*, 4605.
(23) Fan, H. J.; Lee, W.; Scholz, R.; Dadgar, A.; Krost, A.; Nielsch, K.; Zacharias, M. *Nanotechnology* **2005**, *16*, 913.
(24) Kim, D. S.; Hong, R. J.; Fan, H. J.; Bertram, F.; Scholz, R.; Dadgar, A.; Nielsch, K.; Krost, A.; Christen, J.; Gosele, U.; Zacharias, M. *Small* **2007**, *3*, 76.
(25) He, H.; Hsu, J. H.; Wang, C. W.; Lin, H. N.; Chen, L. J.; Wang, Z. L. *J. Phys. Chem. B* **2006**, *110*, 50.
(26) Kim, Y.-J.; Lee, C.-H; Hong, Y. J.; Yi, G.-C; Kim, S. S.; Cheong, H. *Appl. Phys. Lett.* **2006**, *89*, 163128.
(27) Kang, B. S.; Pearton, S. J.; Ren, F. *Appl. Phys. Lett.* **2007**, *90*, 083104.
(28) Weintraub, B.; Deng, Y.; Wang, Z. L. *J. Phys. Chem. C* **2007**, *111*, 10162.
(29) Lee, S. H.; Lee, H. J.; Oh, D.; Lee, S. W.; Goto, H.; Buckmaster, R.; Yasukawa, T.; Matsue, T.; Hong, S.-K; Ko, H. C.; Cho, M.-W.; Yao, T. *J. Phys. Chem. B* **2006**, *110*, 3856.
(30) Kitsomboonloha, R.; Baruah, S.; Myint, M. T. Z.; Subramanian, V.; Dutta, J. *J. Cryst. Growth* **2009**, *311*, 2352.
(31) Aizenberg, J.; Black, A. J.; Whitesides, G. M. *Nature* **1999**, *398*, 495.
(32) Hsu, J. W. P.; Tian, Z. R.; Simmons, N. C.; Matzke, C. M.; Voigt, J. A.; Liu, J. *Nano Lett.* **2005**, *5*, 83.
(33) Qin, D.; Xia, Y.; Whitesides, G. M. *Nat. Protoc.* **2010**, *5*, 491.
(34) Philipsborn, A. C.; Lang, S.; Bernard, A.; Loeschinger, J.; David, C.; Lehnert, D.; Bastmeyer, M.; Bonhoeffer, F. *Nat. Protoc.* **2006**, *1*, 1322.
(35) Wei, M.; Qi, Z.; Ichihara, M.; Honma, I.; Zhou, H. *Nanotechnology* **2007**, *18*, 095608.
(36) Kang, H. W.; Sung, H. J.; Lee, T.-M.; Kim, D.-S.; Kim, C.-J. *J. Micromech. Microeng.* **2009**, *19*, 015025.
(37) Lee, D. H.; Lee, J. A.; Lee, W. J.; Kim, S. O. *Small* **2010**, *7*, 95.